SYSTEM DYNAMIC MODEL AND DESIGN OF A STIRLING PUMP

Anna Winkelmann   Eric J. Barth
Laboratory for the Design and Control of Energetic Systems
Department of Mechanical Engineering
Vanderbilt University, Nashville, TN 37235
eric.j.barth@vanderbilt.edu

ABSTRACT

This paper presents the design and dynamic modeling of a second generation prototype combined Stirling engine pump. The Stirling pump is intended to fill the technological gap of a compact high energy density power supply for untethered fluid power applications in the 50W to 500W range. Specifically, this prototype is intended as a compact and quiet, untethered, hydraulic power supply for an ankle foot orthosis testbed associated with the Center for Compact and Efficient Fluid Power. The energy source for the unit is flexible and can include propane, butane, methane, natural gas, or other high energy density hydrocarbon source of heat. The target output pressure of 7 MPa (1000 psig) is obtained from a pumping stage that is driven by a sealed engine stage that utilizes high pressure helium as the working fluid. The separate pumping stage utilizes the differential pressure swing inside the engine section to pump hydraulic fluid to the desired output pressure. This paper presents the system dynamic model of the Stirling pump, and includes (1) heat transfer from the heat source to the working fluid in the hot space of the engine, (2) heat transfer from the working fluid in the cold space of the engine to the heat sink, (3) energetically derived pressure dynamics in the hot and cold spaces, (4) mass flow around the displacer piston in between the hot and cold sides, (5) work output to the pump driving section, (6) pumping piston inertial dynamics, (7) flow losses through the pump's check valves, and (8) hydraulic power output. This dynamic model allows components of the Stirling pump to be sized. The paper includes results from the dynamic model.

INTRODUCTION

More than 6 million individuals in the US are affected by an impaired ankle function. Commercially available passive Ankle Foot Orthoses (AFO) are compact and durable but lack functionality since they cannot provide active motion control or generate net power. Active AFOs lack utility because they require tethered power supplies. One of the goals of the Center for Compact and Efficient Fluid Power (CCEFP) is to develop a fluid powered untethered device that operates in the 10 to 100 W power range to address the shortcomings of both passive and active AFOs. The Stirling pump is intended to serve as a silent, low vibration, compact, efficient, untethered, and high energy-density hydraulic power supply for an AFO, or similar application.

Stirling engines have been a research curiosity for more than a century. They have the appeal of offering power from any heat source including fuels, solar concentration, biomass, geothermal, or radioisotope decay. They also have the theoretical appeal of offering high thermodynamic efficiency due to the Stirling cycle. In the limited number of applications they have found, Stirling engines have been shown to be reliable and requiring little to zero maintenance. Despite their appealing properties, it is also fair to say that Stirling engines have fallen far short of their expectations primarily due to their low power density.

The historical progression of Stirling machines has offered some improvement in power density as their configurations have progressed from purely kinematic to free-piston varieties. Purely kinematic configurations rely on bulky linkages to enforce the correct phasing between the power piston and the displacer piston. Free-piston Stirling engines rely upon dynamic forces developed in the engine and the dynamic responses of the displacer and power pistons to enforce the necessary relationship between the two. If the engine is designed with these dynamics in mind, it can be shown that kinematic linkages are not necessary [1]. The first purely dynamic (non-kinematic) Stirling engine was Beale's free-piston Stirling engine [1]. The free-piston arrangement was not only lighter, but was able to be hermetically sealed and eliminated side forces on the pistons due to a connecting rod. Moreover, the ability to pressurize a sealed engine allows for higher power densities [2,3].

The challenge with free-piston configurations is to get the phase of the displacer and power piston correct in order to approximate the Stirling cycle. Designing the dynamics to do this correctly and robustly in the face of varying loads and heat

input remains a technological barrier. Some success in the design of working free-piston Stirling engines is represented by many of Beale's arrangements [4, 5], the Harwell Thermomechanical Generator [6, 5, 7], and the liquid piston Fluidyne Stirling engine by West [8, 9]. The analysis of even these *working* Stirling machines demonstrates a knowledge gap with respect to designing their parameters for robust operation [5].

The Stirling pump presented in this paper overcomes this knowledge gap by decoupling the sensitive interacting dynamics of the displacer and power pistons. This is done by directly controlling the motion of the displacer piston. This allows more design degrees of freedom and ensures that the device is insensitive to load or internal dynamics variations. This paper describes the design and dynamic model of the combined Stirling engine pump. The Stirling pump is pre-pressurized and has a separate pump section that uses the pressure swing of the engine to pump hydraulic fluid.

DESIGN OF STIRLING PUMP

The rationale for the design of the proposed device result in large part from results and observations from a previous Stirling Thermocompressor device that was designed, fabricated, and experimentally tested by our research group [10]. The previous (generation 1) device was a multi-stage, true thermocompressor (Fig.1). A true thermocompressor uses the working fluid as the output fluid (air in this case). As discussed below, results from this previous device motivated: 1) a change in architecture from a multistage device to a single stage device, and 2) a change in functionality and architecture from a thermocompressor to a hydraulic pump. A single stage of this previous multistage device is shown in Fig. 2.

The generation 1 device used a brushless DC motor to drive a continuous linear reciprocating lead screw onto which the displacer piston was attached. The displacer piston was chosen to be made from Macor machinable ceramic due to its low thermal conductivity (1.46 W/m/K at 25°C) and its high service temperature. A quartz glass cylinder was chosen to seal the working fluid in between the heater head and the heat sink due to the same characteristics - low thermal conductivity and high service temperature.
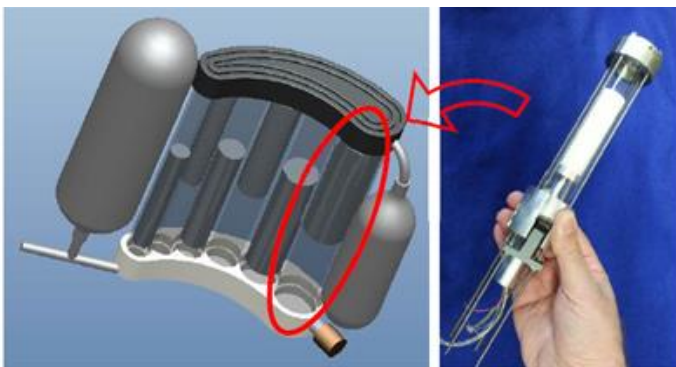

Fig 1. Generation-1 multistage thermocompressor device concept
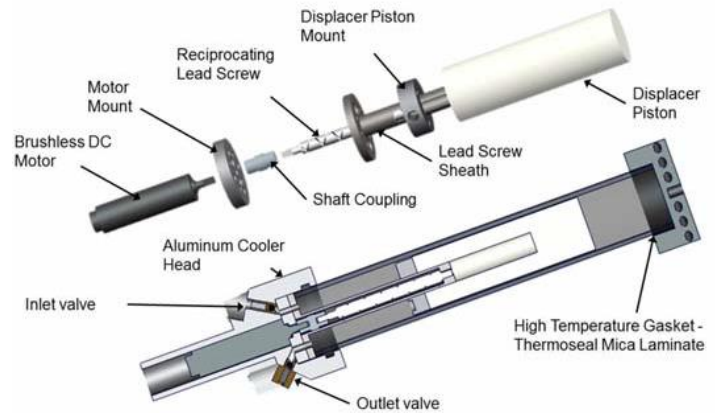

Fig 2. Design of a single stage of the generation-1 thermocompressor device. A reciprocating lead screw driven by a DC motor moves a loose-fit displacer piston between the hot side and the cold side. In response to this, the pressure in the device changes as the working fluid moves between the hot side (high pressure) and the cold side (low pressure). As the pressure fluctuates, the thermocompressor outputs high pressure fluid to a reservoir and intakes low pressure fluid from the environment (or from a previous stage).

MULIT-STAGE TO SINGLE-STAGE DESIGN CHANGE

A dynamic simulation of the multi-stage thermocompressor [10] showed that more than four compression stages would be needed to reach the target output pressure. With respect to the multi-stage architecture, the prospect of having at least four compression stages to reach a target output pressure of 80 psig (for pneumatics reservoir) becomes untenable in the face of the mechanical complexity encountered in our single stage prototype. A multi-stage device requires that each stage become smaller with increasing pressure and the realities of dead-volume in such stages would make them far less than ideal as they become smaller. It was clear that a different approach was needed for the next generation of the device.

The generation 2 device will be of single-stage architecture with a sealed pre-pressurized engine section and separate pumping stage that pumps hydraulic fluid. Although the prospect of a true thermocompressor is appealing, the fundamental work density per stroke [J/(m³stroke)] increases by more than two orders of magnitude by increasing the pre-pressurization (pressure when cold) to 500 psig. This agrees with the observation that almost every Stirling device (actual experimental platform) in the literature operates at a high pressure and agrees with the observations of authors such as G. Walker, G. T. Reader, O.R. Fauvel, I. Urieli, N. Isshiki, D. Gedeon, M. B. Ibrahim, M. Carlini, L. Bauwens, and others. Pursuing this pre-pressurized architecture, as opposed to a true thermocompressor, requires a separate pump section that utilizes the differential pressure swing inside the engine section. Based on the experimentally measured heat transfer and pressure ratio of the generation-1 device, an output pressure of greater than 1000 psig (7000 kPa) can be obtained by utilizing a separate pumping stage and a single pre-pressurized sealed engine section with a similar size as the generation-1 device.

WORKING FLUID AND PUMPING FLUID

As discussed above, better compactness and power density can be achieved by using a single-stage, pre-pressurized engine section. This design change allows a consideration of a different working fluid than air. For maximum efficiency and power, helium was selected as the working fluid in the sealed engine section. The advantage of helium over air is that helium has a higher heat transfer coefficient than air. For our conditions, the use of helium over air would result in a 20 times higher heat transfer coefficient (14800 $W/m^2/K$ for helium vs. 715 $W/m^2/K$ for air).
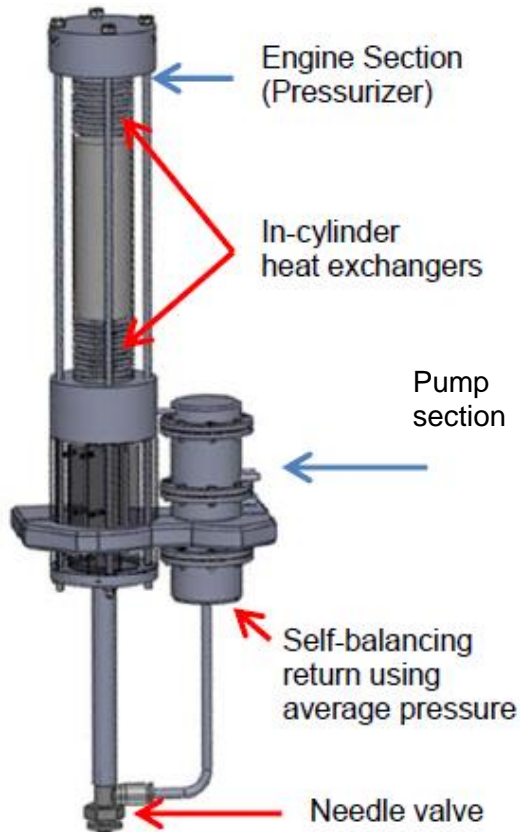

Fig 3. Design of the generation 2 device

The design change to a sealed single-stage also allows for a consideration of the fluid being pumped to be something other than air. Hydraulic pumping is inherently more efficient than compressing and pumping air. This is due to the fact that when air is compressed, appreciable energy is stored as pressure potential energy that can be lost in the form of heat once pumped to its destination. Driving an air compressor also presents the possibility of pressurizing the gas to an inadequate level to pump, and then losing the work that was needed for that pressurization. This occurs even in the case where some of the air is pumped and may leave a remainder that is not pumped due to dead volume in the compressor section. This remainder is then susceptible to heat loss. Due to hydraulic oil's much higher stiffness as compared to a gas, much less energy is stored in the compression of the fluid thereby reducing thermal

effects during the pumping phase. Finally, since hydraulic fluid is nearly incompressible, it eliminates the dead volume in the pumping section.

The design of the separate pump stage can be seen in Figure 4. The pump section utilizes the differential pressure swing inside the engine section to pump hydraulic fluid at a desired output pressure. The pump section is composed of three types of chambers; the driving chamber, the pumping chamber, and the return chamber. The driving chamber will be connected to the cold side of the engine section such both are always at the same pressure. The bottom chamber represents a self-balancing return chamber. This is achieved by staying near an average pressure via a flow restriction implemented with a simple needle valve (see Fig. 3). The pressure difference in the driving and return chamber will cause the piston in the pumping chamber to move. When the pressure in the driver chamber is higher than in the return chamber, the piston moves down and pumps the hydraulic fluid in the lower pumping chamber through a check valve when the pressure is greater than the supply pressure. Simultaneously, the fluid in the upper pumping chamber decompresses and ultimately draws in more fluid through a check valve from the low pressure side of the hydraulic system. Conversely, when the piston moves up, fluid is pumped out of the upper pumping chamber and drawn in to the lower pumping chamber.
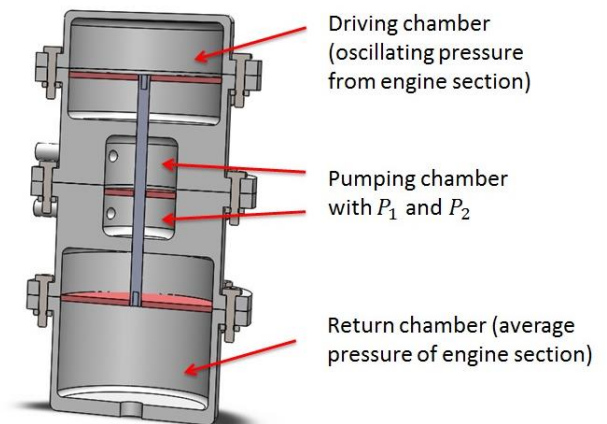

Fig 4. Pumping Section

OTHER DESIGN CHANGES

Other design changes that need to be made to the generation-1 device include a different driver mechanism for the displacer piston and a different sealing mechanism at the hot end. For the generation 1 device, the position and velocity of the displacer was controlled by driving a reciprocating lead screw with a brushless DC motor. The reciprocating lead screw had "criss-crossed' left-handed and right-handed threads which enabled the motor to be driven in one direction while achieving a reciprocating motion of the displacer piston. This was intended to reduce the power consumption of the motor since it does not need to accelerate and decelerate the motor shaft. Nevertheless, the power consumption was still found to be much higher than expected due to excessive friction in the lead

screw mechanism. As a result, the displacer of the generation 1 device could only be driven at a frequency of 2.8 Hz. Dead volume around the lead screw mechanism was also a downside of the mechanism and limited the pressure swing in the engine. At 800°C and 2.8 Hz, the generation-1 device showed a pressure ratio of 1.6. While favorably comparable to devices in the literature, it was lower than expected.

The dead-volume and the higher than expected motor power necessitated a better solution for the linear drive mechanism of the displacer piston. The generation 2 device replaces the DC motor and the reciprocating lead-screw with a compact COTS linear actuator (Faulhaber) (see Fig 5). The linear DC-Servomotor is light weight and has linear Hall sensors for position sensing. The positioning of the rod can be controlled very accurately such that dead volume at the cylinder ends can be held to a minimum. The smooth shaft of the linear motor also reduces the dead volume seen in the reciprocating lead screw design. A linear spring located in between the displacer piston and the linear motor will act as a conservative restoring force to minimize actuation energy, and effectively replaces the energetically motivated unidirectional operation of the reciprocating lead screw.

Fig 5. Linear DC Servomotor

Finally, experimental results of the generation-1 device revealed a slow leak resulting from the high temperature seal between the fused quartz glass and the heater head. To avoid a leak, the generation 2 device will have an engine cylinder made of Inconel 625 as opposed to fused quartz. This will be tougher and able to be welded, thus solving the sealing problem at the hot end.

DYNAMIC MODEL

The entire Stirling Pump can be dynamically modeled as having two sections, namely, the engine section and the pump section. The only input to the pump section is the pressure swing on the cold side of the engine section. The displacer piston in the engine section is driven by a linear DC servomotor with a sinusoidal velocity of

$$V = l_{Stroke} \pi f \sin(2\pi f t) \quad (1)$$

where f is the frequency the displacer motion, and l_{Stroke} is the stroke length of the displacer piston in the engine section of the Stirling pump. The position of the displacer is given accordingly by:

$$x_{displacer} = \frac{l_{stroke}}{2} + \frac{l_{stroke}}{2}\cos(2\pi f t) \quad (2)$$

The engine section of the Stirling pump is modeled as two control volumes of variable size. The control volumes represent the volume of the medium in the hot and the cold side of the engine section. The two control volumes are separated by the displacer piston which represents a flow restriction. The size of the control volume and the rate at which these are changing are governed by the position and velocity of the displacer piston above. The walls in the hot control volume (V_h) transfer thermal energy from heat source to the medium, and the walls in the cold control volume (V_k) transfer thermal energy from the medium out of the engine section of the Stirling pump. The wall temperatures on the hot and cold side of the engine section are set to a constant temperature of T_h and T_k, respectively. The dead volume around the displacer piston is equally divided into the model of V_h and V_k. Since the displacer never hits the ends of the cylinder, additional dead volume is added to both sides.

The pressure dynamics in the cylinder were derived from a fundamental power balance of the stored energy, enthalpy, heat flow and work:

$$\dot{U} = \dot{H} + \dot{Q}_{heat} - \dot{W} \quad (3)$$

Rearranging the terms and solving for the pressure dynamics inside the control volume yields:

$$\dot{P} = \frac{\sum \dot{m}\gamma_{He}RT_{flow} - \gamma_{He}P\dot{V} + h_{He}A_{h,k}(\gamma_{He}-1)(T_{wall,h,k}-T)}{V} \quad (4)$$

An estimate of the heat transfer coefficient h_{He} was done by using fully developed pipe flow analysis as similar to [11]. In order to determine whether the flow is laminar or turbulent, the Reynolds number was calculated:

$$\mathrm{Re} = \frac{\dot{x}_m \delta}{\nu} \quad (5)$$

where $\dot{x}_m$ is the mean velocity of helium, δ is the characteristic length, and ν is the kinematic viscosity of helium. The hydraulic diameter was used for the characteristic length given by:

$$\delta = \frac{4A_c}{C} \quad (6)$$

where A_c is the area of the gap in between the engine cylinder and the displacer piston and C is the wetted perimeter given by:

$$C = \pi(d_{cylinder} - d_{displacer}) \quad (7)$$

where $d_{cylinder}$ is the inside diameter of the Inconel housing and $d_{displacer}$ is the diameter of the displacer piston.

The heat transfer coefficient is determined by calculating the Nusselt number and solving for the heat transfer coefficient h by using the following equation:

$$Nu = \frac{h\delta}{k} = a \cdot \mathrm{Re}^m \cdot Pr^n \quad (8)$$

where k is the thermal conductivity, Pr is the Prandtl number and a, m, n are constants that depend on the flow regime. For a

frequency of 20 Hz, turbulent flow (Re>2300), and a smooth pipe, the constants used in the implementation of equations 5-8 are shown in the Table 1 below. Solving for the heat transfer coefficient yields 14800 W/m²/K. Since the calculation of this parameter depends on the mean pressure and the mean temperature in determining the kinematic viscosity, conservative values were used such that the h calculated is a lower bound for the conditions in the engine.

Table 1: values of significant parameters

$\dot{x}_m$	125 m/s
δ	0.00099 m
v	5.643e-6 m²/s
k	0.245 W/m/K
a	0.023 [11]
Pr	0.656
m	0.8 [11]
n	0.3 [11]
h	14800 W/m²/K

The mass flow restriction between the displacer piston and the Inconel cylinder that separates the two control volumes was modeled using Grinnel's model of compressible fluid flow [12] in a thin passage, which is given by:

$$\dot{m} = \left(\frac{r_{piston}s^3}{12\mu_{helium}RT_{flow}L_{piston}} \right)\left(P_u^{\;2} - P_d^{\;2} \right) \qquad (9)$$

where P_u and P_d are the upstream and downstream pressures found in the control volumes.

The constants used in the implementation of Equations 4 and 9 are shown in Table 2.

Table 2: Values of significant parameters

$s = 0.5$ mm	$R = 2.07\text{x}10^9$ uJ/kg/K
$L_{piston} = 76.2$ mm	$r_{piston} = 24.5$ mm
$\gamma_{helium} = 1.664$	$T_{wall,\,h} = 550$ºC
$T_{wall,\,k} = 50$ºC	$\mu_{helium} = 2.8\text{x}10^{-8}$ Ns/m
$h_{helium} = 14800$ W/m²/K	

The piston position and velocity in the pumping chamber depend on the cross-sectional area of the driving/return chamber (A_d), the pressure swing inside the engine, the cross-

sectional area of the pumping chamber (A_p) and the pressure in both pumping chambers. The equation of motion is

$$M\ddot{x} = P_k A_d + P_1 A_p - P_2 A_p - P_{avg}A_d - b\dot{x} \qquad (10)$$

where M is the mass of the piston/rod assembly in the pumping section, P_k is the pressure in the driving chamber, P_{avg} is the pressure in the return chamber, P_1 and P_2 are the pressures in the upper and lower pumping chamber respectively, and b is a damping coefficient resulting from the viscous friction of the piston and rod.

The equation for the volumetric flow rate through a small cross-sectional area was used to determine the pressure P_1 and P_2. The volumetric flow rate is given by:

$$Q = A_v \sqrt{\frac{2}{\rho\varepsilon}(P_u - P_d)} \qquad (11)$$

where A_v is the cross-sectional area of the valve opening, ρ is the density of the fluid, and ε is the dimensionless loss coefficient. Dependent on the direction the piston is moving, the upstream pressure and the downstream pressure are selected according to Table 3.

Table 3: conditions for P_u and P_d

	sign of Q	Pumping chamber	P_u	P_d
$\dot{x} > 0$	-1	lower	P_2 via Eq. 12	P_s
$\dot{x} > 0$	1	upper	P_{atm}	P_1 via Eq. 13
$\dot{x} < 0$	1	lower	P_{atm}	P_2 via Eq. 13
$\dot{x} < 0$	-1	upper	P_1 via Eq. 12	P_s

The negative sign for the volumetric flow rate indicates that fluid is being pumped out of the pumping section while a positive sign indicates that fluid is pumped into the pumping section. By calculating the flow rate Q with the equation $Q = \dot{x}A_p$ and then setting P_u and P_d to the boundary conditions indicated in Table 3, the pressures in the upper and lower pumping chambers P_1 and P_2 can be found.

$$P_u = \left(\frac{\dot{x}A_p}{A_v} \right)^2 \frac{\rho\varepsilon}{2} + P_d \qquad (12)$$

$$P_d = P_u - \left(\frac{\dot{x}A_p}{A_v} \right)^2 \frac{\rho\varepsilon}{2} \qquad (13)$$

These dynamics fully describe the engine and pump section of the Stirling device. To further characterize the device, average output power is calculated by filtering the instantaneous power with a slow, unity-gain first order filter. The instantaneous power output $\mathbf{P}_{instant}$ is calculated by:

$$\mathbf{P}_{instant} = Q_{out} P_s \qquad (14)$$

where $Q_{out} = A_p|\dot{x}|$ is the volumetric flow rate out of the two pumping chambers and P_s is the desired supply pressure.

RESULTS

Results of the dynamic simulation show that the device can pump 1000 psig (7000 kPa) when the engine runs at 20 Hz (controlled sinusoidal motion of the displacer as given by Eqn. 2), is initially pressurized to 500 psig (3.55 MPa) with cold helium and is then held at a constant temperature T_h of 550°C on the hot side. The parameters for the Stirling pump as designed are given in Table 4.

Table 4: Parameters used in Simulation

l_{cyl}	200 mm	l_{drive}	22 mm
$d_{cylinder}$	50 mm	$bore_{drive/return}$	60 mm
l_{piston}	76 mm	$bore_{pump}$	10 mm
d_{piston}	49 mm	d_{valve}	2.5 mm
		M	0.2 kg
		b	500 Ns/m

The pressure difference in the driving and return chamber (Fig. 6) caused by the pressure swing inside the engine results in a displacement of the pumping piston as seen in Figure 7.
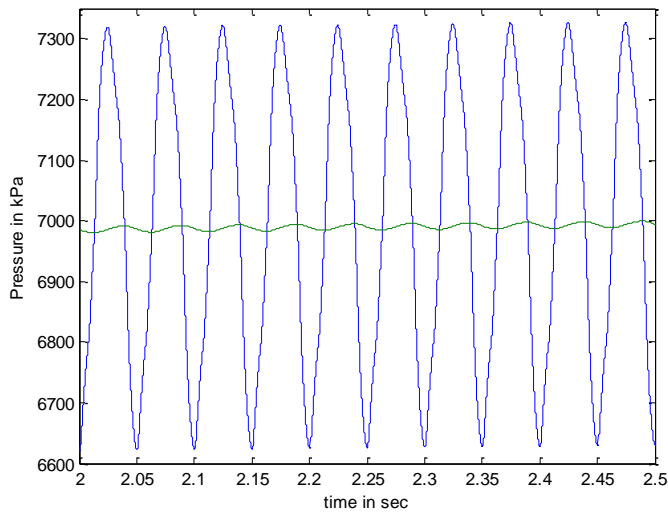

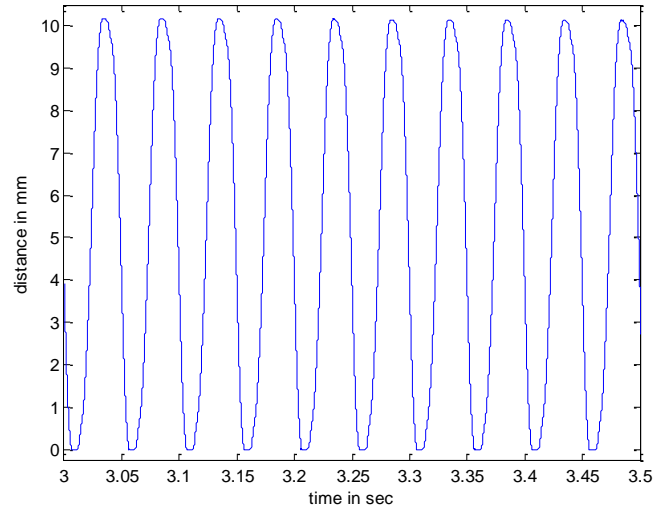Fig 6. Driving (blue) and average (green) pressure vs. time

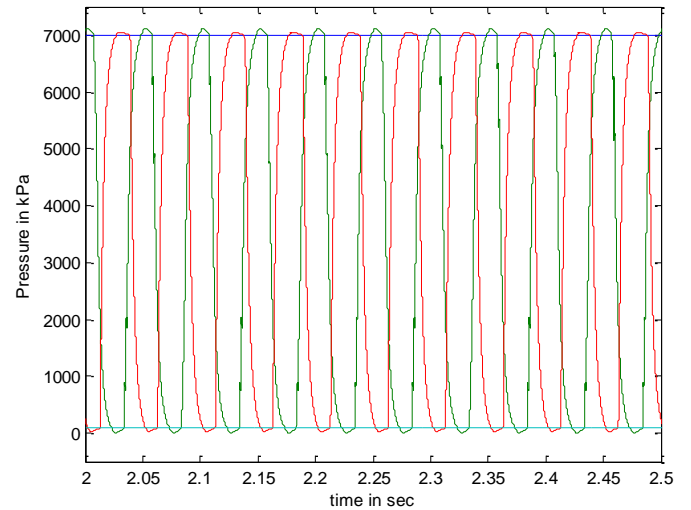Fig 7. Displacement of the pumping piston with respect to time

Fig 8. Pressure dynamics in the pumping chamber compared to the supply pressure (7 MPa) and atmospheric pressure (101 kPa)

The pumping piston moves up and down in response to the engine and load pressures with a maximum displacement of about 10 mm. The pressure inside the pumping section is governed by the piston's velocity according to Equations 12 and 13 and under the conditions shown in Table 3. Figure 8 shows the pressure dynamics of P_1 and P_2 compared to supply and atmospheric pressure. If the pressure in either pumping chamber is greater than supply pressure, hydraulic fluid is pumping out of the pumping chamber. Conversely, if the pressure is below atmospheric pressure, hydraulic fluid is pumped into the pumping chamber. This is captured compactly as $Q_{out} = A_p|\dot{x}|$. An average power output of about 230 W can be achieved when operated at 20 Hz with a cold helium pre-pressurization of 500 psig.

CONCLUSION

In this paper the design and dynamic model of a second generation prototype Stirling pump is described. Taking into account observations and results from the generation 1 device, the proposed design changes for generation 2 are presented and justified. The heat transfer coefficient was greatly improved by using helium as the working fluid in the sealed pre-pressurized engine section. Simulation results are used to size the dimensions of the Stirling pump to achieve a high output power. A single-stage unit fulfills the energetic requirements set by the CCEFP for the Stirling pump of a hydraulic output power of 1000 psig and an average supply power ranging between 50W to 500W. The new design can greatly improve output power of the generation 1 device. Future work will formulate a controller for the efficient and precise oscillation of the displacer piston, build and run the engine/pump device, and validate the model with experimental data.

ACKNOWLEDGEMENT

REFERENCES

[1] G. Walker, G. Reader, O. R. Fauvel, E. R. Bingham, *The Stirling Alternative: Power Systems, Refrigerants and Heat Pumps*, Gordon and Breach Science Publishers, 1994.

[2] G. Walker, "Large Free-Piston Stirling Engines," *Lecture Notes in Engineering*, Springer-Verlag, pp.216-221, 1985.

[3] A. J. Organ, *The Regenerator and the Stirling Engine*, Mechanical Engineering Publications Limited, London, 1997.

[4] G. Walker, Stirling Engines, Oxford University Press, 1980.

[5] G. Walker and J. R. Senft, *Lecture Notes in Engineering: Free Piston Stirling Engines*, Springer-Verlag, New York, 1985.

[6] E. H. Cooke-Yarborough, E. Franklin, T. Gesow, R. Howlett, C. D. West, "Thermomechanical generator – an Efficient Means of Converting Heat to Electricity at Low Power Levels," *Proceedings of the IEE*, no. 121, p. 749-751.

[7] C. D. West, *Principles and Applications of Stirling Engines*, Van Nostrand Reinhold Company, New York, 1986.

[8] C. D. West, *Liquid Piston Stirling Engines*, Van Nostrand Reinhold Company, New York, 1983.

[9] G. T. Reader and M. A. Clarke, "Liquid Piston Stirling Air Engines," *2nd International Conference on Stirling Engines*, 14p, 1984.

[10] M. E. Hofacker, N. Kumar, E. J. Barth. "Dynamic Simulation and Experimental Validation of a Single Stage Thermocompressor for a Pneumatic Anke-Foot Orthosis". *2013 Proceedings of the 25th Symposium on Fluid Power and Motion Control, ASME/Bath, FPMC2013-4483*, October 6-9, 2013, Sarasota, FL.

[11] J. Van de Ven, P. Gaffuri, B. Mies, and G. Cole, "Developments Towards a Liquid Piston Stirling Engine," *International Energy Conversion Engineering Conference*, Cleveland, Ohio, 2008.

[12] S. K. Grinnell, "Flow of a Compressible Fluid in a Thin Passage". *ASME*, 16 pages, 1954.